11196 *Inorg. Chem.* **2009**, *48*, 11196–11208
DOI: 10.1021/ic901662z

Inorganic Chemistry
Article

Structures, Metal Ion Affinities, and Fluorescence Properties of Soluble Derivatives of Tris((6-phenyl-2-pyridyl)methyl)amine

Jian Liang,[†] Jing Zhang,[†] Lei Zhu,[†] Alexander Duarandin,[†] Victor G. Young, Jr.,[‡] Nicholas Geacintov,*[,†] and James W. Canary*[,†]

[†]*Department of Chemistry, New York University, New York, New York 10003, and* [‡]*Department of Chemistry, University of Minnesota, 207 Pleasant Street, South East, Minneapolis, Minnesota 55455*

Received August 19, 2009

Metal complexes of tris((6-phenyl-2-pyridyl)methyl)amine (**2**) have hydrophobic cavities that potentially accommodate small molecules. However, the utility of this attractive motif has been hampered by the poor solubility of such complexes in many common solvents. In this study, two tripodal ligands (**3**, tris-[6-(3,4,5-trimethoxy-phenyl)-pyridin-2-ylmethyl]-amine, and **4**, tris((6-(3,4,5-tris(2-(2-(2-methoxyethoxy)ethoxy)ethoxy)phenyl)pyridin-2-yl)methyl)amine) derived from **2** were prepared with enhanced solubility in organic and aqueous solvents. The X-ray crystallographic analyses of selected ligands and complexes revealed that the hydrophobic cavities inside the zinc complexes were retained after derivatization. Fluorescence, nuclear magnetic resonance (NMR), and potentiometric titration studies, which were enabled by the improved solubility, were performed to investigate the binding properties of the soluble ligands (**3** and **4**) with metal ions such as Zn^{2+} and Cu^{2+}. When saturating quantities of Zn^{2+} ions are added to ligand **3** in acetonitrile, the fluorescence emission maximum exhibits a pronounced red shift of ~80 nm (from 376 to 457 nm) and is enhanced by a factor of >100 when measured at 520 nm. The fluorescence properties of the Zn^{2+} ion-coordinated ligands in the Zn(**3**) complex are consistent with a charge-transfer character in the excited state, with possible contributions from a planarization of the pyridyl-trimethoxyphenyl groups in the excited state, and from excitonic interactions.

Introduction

The mechanisms of interaction of metal ions with organic ligands that change the fluorescence properties of the latter have been of great interest because of the potential for improving the sensitivities and selectivities of metal ion probes. Some of the general principles of metal cation binding and their recognition by fluorescence-emitting sensors have been reviewed.[1] A number of examples of Zn^{2+}−organic ligand complexes have been reported that exhibit red-shifted fluorescence bands. For example, Ajayaghosh et al. noted that the titration of a flexible bipyridyl derivative with Zn^{2+} ions changed the fluorescence emission maximum of the free ligand from 407 to 450 nm in the Zn complex and attributed this shift to a coplanarization of the two pyridyl aromatic rings.[2] Pina et al. studied the formation of complexes of Zn^{2+} ions with a cyclic polyaminic macrocyclic structure containing two phenanthroline units bearing two naphthalene moieties at both ends; a prominent red shift in the fluorescence spectrum of this Zn^{2+} ion−ligand complex was attributed to an intramolecular excimer emission arising from the interaction of one phenanthroline unit in the excited state with another phenanthroline unit in the ground state.[3] The binding of Zn^{2+} ions to a macrocyclic phenanthrolinophane derivative bearing a pendant arm containing a coordinating amine and an anthracene aromatic ring system resulted in a red-shifted emission in ethanol solution due to exciplex formation between a phenanthroline and an anthracene moiety.[4] Both red-shifted absorption and fluorescence bands have been observed with other ligands and attributed to charge-transfer (CT) states upon Zn^{2+} ion binding to a terpyridine electron acceptor and a diphenylaminophenyl electron donor moiety in ethanol, [5] or a substituted phenyl or biphenyl electron donor group in acetonitrile,[6] and pyrene−terpyridine conjugates in buffered aqueous solution.[7] An analogous CT mechanism was invoked to

*To whom correspondence should be addressed. E-mail: nicholas.geacintov@nyu.edu (N.E.G.), james.canary@nyu.edu (J.W.C.).

(1) (a) Valeur, B.; Leray, I. *Coord. Chem. Rev.* **2000**, *205*, 3–40. (b) Dai, Z.; Canary, J. W. *New J. Chem.* **2007**, *31*, 1708–1718. (c) Que, E. L.; Domaille, D. W.; Chang, C. J. *Chem. Rev.* **2008**, *108*, 1517–1549.

(2) Ajayaghosh, A.; Carol, P.; Sreejith, S. *J. Am. Chem. Soc.* **2005**, *127*, 14962–14963.

(3) Pina, J.; de Melo, J. S.; Pina, F.; Lodeiro, C.; Lima, J. C.; Parola, A. J.; Soriano, C.; Clares, M. P.; Albelda, M. T.; Aucejo, R.; Garcia-Espana, E. *Inorg. Chem.* **2005**, *44*, 7449–7458.

(4) Bencini, A.; Berni, E.; Bianchi, A.; Fornasari, P.; Giorgi, C.; Lima, J. C.; Lodeiro, C.; Melo, M. J.; de Melo, J. S.; Parola, A. J.; Pina, F.; Pina, J.; Valtancoli, B. *Dalton Trans.* **2004**, 2180–2187.

(5) Goodall, W.; Williams, J. A. G. *Chem. Commun.* **2001**, 2514–2515.

(6) Li, Y. Q.; Bricks, J. L.; Resch-Genger, U.; Spieles, M.; Rettig, W. *J. Phys. Chem. A* **2006**, *110*, 10972–10984.

(7) Peng, X.; Xu, Y.; Sun, S.; Wu, Y.; Fan, J. *Org. Biomol. Chem.* **2007**, *5*, 226–228.

 Published on Web 10/30/2009

account for the appearance of a broad, structureless, red-shifted fluorescence mechanism when an aromatic iminodiacetate electron acceptor, connected to an anthracene fluorophore by covalent methylene spacers, was titrated with Zn^{2+} ions in aqueous solutions. Other types of ratiometric Zn^{2+} ion sensors with red-shifted fluorescence emission spectra associated with a deprotonation mechanism have been reported using 6,7-dihydroxycoumarin and 1,2-dihydroxyanthraquinone as a ligand in 75% methanol−aqueous buffer solutions[8] and an excited state intramolecular transfer mechanism in the case of 2-(2′-benzene-sulfonamidophenyl)benzimidazole ligand in aqueous solutions.[9]

Tris(2-pyridylmethyl)amine (TPA, **1**), which possesses four nitrogen atoms for the ligation of a wide variety of metal ions, has been studied extensively.[10] Many derivatives of TPA have also been described, including tris((6-methyl-2-pyridyl)methyl)amine,[11] tris((6-amino-2-pyridyl)methyl)-amine,[12] tris(2,2′-bipyridin-6-ylmethyl)amine,[13] and tris(2-quinolylmethyl)amine.[14] Studies of TPA-based tripodal complexes have included metalloprotein models,[15] catalysis,[16] molecular recognition,[17] and sensing.[18] We previously studied several TPA derivatives in which interactions between the arms of the ligand resulted in excitonic interactions.[19] We have recently reported that a derivative of TPA that contains an 8-hydroxyquinaldine moiety in one arm forms a highly fluorescent 1:1 complex with Zn^{2+} in solution.[20] Here we have synthesized other derivatives of TPA and explored the spectroscopic characteristics of Zn^{2+} ion complexes with compound **3**.

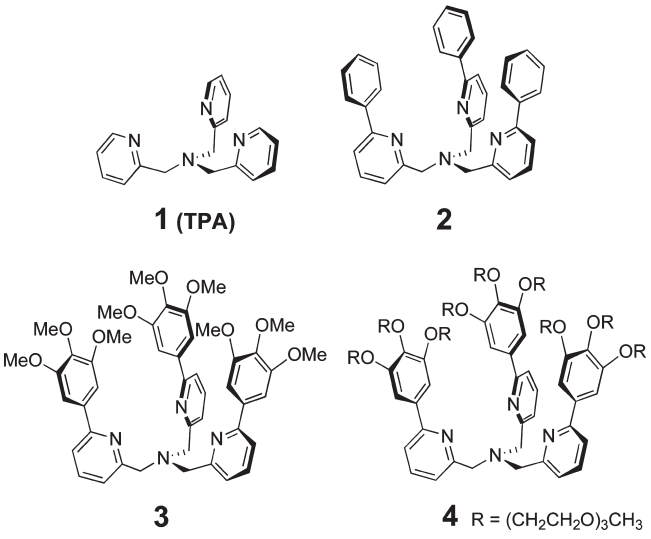

Phenyl-substituted TPA derivatives have been studied including PhTPA, Ph_2TPA, and tris((6-phenyl-2-pyridyl)methyl)amine (Ph_3TPA, **2**).[21,22] Our previous work[21g−i]

(8) Zhang, L.; Dong, S.; Zhu, L. *Chem. Commun*. **2007**, 1891–1893.
(9) Henary, M. M.; Wu, Y. G.; Fahrni, C. J. *Chem.—Eur. J*. **2004**, *10*, 3015–3025.
(10) (a) Natrajan, L.; Pecaut, J.; Mazzanti, M.; LeBrun, C. *Inorg. Chem*. **2005**, *44*, 4756–4765. (b) Tajika, Y.; Tsuge, K.; Sasaki, Y. *Dalton Trans*. **2005**, 1438–1447. (c) Davies, C. J.; Solan, G. A.; Fawcett, J. *Polyhedron* **2004**, *23*, 3105–3114. (d) Mukhopadhyay, U.; Bernal, I.; Massoud, S. S.; Mautner, F. A. *Inorg. Chim. Acta* **2004**, *357*, 3673–3682. (e) Yamada, T.; Shinoda, S.; Sugimoto, H.; Uenishi, J.-I.; Tsukube, H. *Inorg. Chem*. **2003**, *42*, 7932–7937. (f) Robertson, N.; Carney, M. J.; Halfen, J. A. *Inorg. Chem*. **2003**, *42*, 6876–6885. (g) Hazell, A.; McGinley, J.; Toftlund, H. *Inorg. Chim. Acta* **2001**, *323*, 113–118. (h) Xu, L.; Sasaki, Y.; Abe, M. *Chem. Lett*. **1999**, 163–164. (i) Canary, J. W.; Wang, Y.; Roy, R., Jr.; Que, L., Jr.; Miyake, H. *Inorg. Synth*. **1998**, *32*, 70–75. (j) Anderegg, G.; Wenk, F. *Helv. Chim. Acta* **1967**, *50*, 2330–2332. (k) Paine, T. K.; Costas, M.; Kaiser, J.; Que, L., Jr. *J. Biol. Inorg. Chem*. **2006**, 272–276.
(11) (a) Zhang, Z.−H.; Ma, Z.-H.; Tang, Y.; Ruan, W.-J. *J. Chem. Crystallogr*. **2004**, *34*, 119–125. (b) Zhang, Z.-H.; Bu, X.-H.; Ma, Z.-H.; Bu, W.-M.; Tang, Y.; Zhao, Q.-H. *Polyhedron* **2000**, *19*, 1559–1566. (c) Bebout, D. C.; Bush, J. F., II; Crahan, K. K.; Bowers, E. V.; Butcher, R. J. *Inorg. Chem*. **2002**, *41*, 2529–2536. (d) Bebout, D. C.; Bush, J. F., II; Crahan, K. K.; Kastner, M. E.; Parrish, D. A. *Inorg. Chem*. **1998**, *37*, 4641–4646. (e) Shiren, K.; Fujinami, S.; Suzuki, M.; Uehara, A. *Inorg. Chem*. **2002**, *41*, 1598–1605. (f) Hetterscheid, D. G. H.; Kaiser, J.; Reijerse, E.; Peters, T. P. J.; Thewissen, S.; Blok, A. N. J.; Smits, J. M. M.; de Gelder, R.; de Bruin, B. *J. Am. Chem. Soc*. **2005**, *127*, 1895–1905.
(12) (a) Mareque-Rivas, J. C.; Prabaharan, R.; Martin de Rosales, R. T.; Metteau, L.; Parsons, S. *Dalton Trans*. **2004**, 2800–2807. (b) Mareque-Rivas, J. C.; Prabaharan, R.; Parsons, S. *Dalton Trans*. **2004**, 1648–1655. (c) Mareque-Rivas, J. C.; Prabaharan, R.; Martin de Rosales, R. T. *Chem. Commun*. **2004**, 76–77. (d) Wada, A.; Honda, Y.; Yamaguchi, S.; Nagatomo, S.; Kitagawa, T.; Jitsukawa, K.; Masuda, H. *Inorg. Chem*. **2004**, *43*, 5725–5735. (e) Jitsukawa, K.; Harata, M.; Arii, H.; Sakurai, H.; Masuda, H. *Inorg. Chim. Acta* **2001**, *324*, 108–116. (f) Berreau, L. M. *Eur. J. Inorg. Chem*. **2006**, 273–283.
(13) (a) Wietzke, R.; Mazzanti, M.; Latour, J.-M.; Pecaut, J. *J. Chem. Soc., Dalton Trans.: Inorg. Chem*. **1998**, 4087–4088. (b) Ziessel, R.; Lehn, J. M. *Helv. Chim. Acta* **1990**, *73*, 1149–1162. (c) Lehn, J. M.; Ziessel, R. *Chem. Commun*. **1987**, 1292–1294.
(14) (a) Zhang, J.; Siu, K.; Lin, C. H.; Canary, J. W. *New J. Chem*. **2005**, *29*, 1147–1151. (b) Kryatov, S. V.; Taktak, S.; Korendovych, I. V.; Rybak-Akimova, E. V.; Kaizer, J.; Torelli, S.; Shan, X.; Mandal, S.; MacMurdo, V.; Mairata i Payeras, A.; Que, L., Jr. *Inorg. Chem*. **2005**, *44*, 85–99. (c) Wei, N.; Murthy, N. N.; Karlin, K. D. *Inorg. Chem*. **1994**, *33*, 6093–6100. (d) Wei, N.; Murthy, N. N.; Chen, Q.; Zubieta, J.; Karlin, K. D. *Inorg. Chem*. **1994**, *33*, 1953–1965. (f) Zhang, J.; Canary, J. W. *Org. Lett*. **2006**, *8*, 3907–3910.
(15) (a) Wasser, I. M.; Martens, C. F.; Verani, C. N.; Rentschler, E.; Huang, H.-W.; Moënne-Loccoz, P.; Zakharov, L. N.; Rheingold, A. L.; Karlin, K. D. *Inorg. Chem*. **2004**, *43*, 651–662. (b) Jensen, M. P.; Lange, S. J.; Mehn, M. P.; Que, E. L.; Que, L., Jr. *J. Am. Chem. Soc*. **2003**, *125*, 2113–2128. (c) Yamaguchi, S.; Tokairin, I.; Wakita, Y.; Funahashi, Y.; Jisukawa, K.; Masuda, H. *Chem. Lett*. **1997**, *32*, 406–407.
(16) (a) de Campo, F.; Lastécouères, D.; Verlhac, J.-B. *Chem. Commun*. **1998**, 2117–2118. (b) Chen, K.; Que, L., Jr. *Angew. Chem., Int. Ed*. **1999**, *38*, 2227–2229.
(17) (a) Canary, J. W.; Allen, C. S.; Castagnetto, J. M.; Chuang, C.-L.; Lajmi, A. R.; dos Santos, O.; Xu, X. In *Molecular Recognition and Inclusion*; Coleman A. W., Ed.; Kluwer Academic Publishers: Dordrecht, The Netherlands, 1998; pp 179−184.(b) Canary, J. W.; Zahn, S.; Chiu, Y.-H.; dos Santos, O.; Liu, J.; Zhu, L. *Enantiomer* **2000**, *5*, 397–403.
(18) (a) Tobey, S. L.; Anslyn, E. V. *Org. Lett*. **2003**, *5*, 2029–2031. (b) Yamada, T.; Shinoda, S.; Tsukube, H. *Chem. Commun*. **2002**, 1218–1219.
(19) (a) Canary, J. W. *Chem. Soc. Rev*. **2009**, *38*, 747–756. (b) Zahn, S.; Canary, J. W. *J. Am. Chem. Soc*. **2002**, *124*, 9204–9211.
(20) Royzen, M.; Durandin, A.; Young, V. G.; Geacintov, N. E.; Canary, J. W. *J. Am. Chem. Soc*. **2006**, *128*, 3854–3855.
(21) (a) Dai, Z.; Proni, G.; Mancheno, D.; Karimi, S.; Berova, N.; Canary, J. W. *J. Am. Chem. Soc*. **2004**, *26*, 11760–11761. (b) Zhu, L.; Dos Santos, O.; Koo, C. W.; Rybstein, M.; Pape, L.; Canary, J. W. *Inorg. Chem*. **2003**, *42*, 7912–7920. (c) Xu, X.; Maresca, K. J.; Das, D.; Zahn, S.; Zubieta, J.; Canary, J. W. *Chem.—Eur. J*. **2002**, *8*, 5679–5683. (d) Dai, Z.; Xu, X.; Canary, J. W. *Chem. Commun*. **2002**, 1414–1415. (e) Canary, J. W.; Allen, C. S.; Castagnetto, J. M.; Chiu, Y.-H.; Toscano, P. J.; Wang, Y. *Inorg. Chem*. **1998**, *37*, 6255–6262. (f) dos Santos, O.; Lajmi, A. R.; Canary, J. W. *Tetrahedron Lett*. **1997**, *38*, 4383–4386. (g) Chuang, C.-L.; dos Santos, O.; Xu, X.; Canary, J. W. *Inorg. Chem*. **1997**, *36*, 1967–1972. (h) Chuang, C.-L.; Lim, K.; Canary, J. W. *Supramol. Chem*. **1995**, *5*, 39–43. (i) Chuang, C.-L.; Lim, K.; Chen, Q.; Zubieta, J.; Canary, J. W. *Inorg. Chem*. **1995**, *34*, 2562–2568.
(22) (a) Jensen, M. P.; Mehn, M. P.; Que, L., Jr. *Angew. Chem., Int. Ed*. **2003**, *42*, 4357–4360. (b) Jensen, M. P.; Lange, S. J.; Mehn, M. P.; Que, E. L.; Que, L., Jr. *J. Am. Chem. Soc*. **2003**, *125*, 2113–2128. (c) Lange, S. J.; Miyake, H.; Que, L., Jr. *J. Am. Chem. Soc*. **1999**, *121*, 6330–6331. (d) Rudzka, K.; Makowska-Grzyska, M. M.; Szajna, E.; Arif, A. M.; Berreau, L. M. *Chem. Commun*. **2005**, 489–491. (e) Szajna, E.; Dobrowolski, P.; Fuller, A. L.; Arif, A. M.; Berreau, L. M. *Inorg. Chem*. **2004**, *43*, 3988–3997. (f) Makowska-Grzyska, M. M.; Szajna, E.; Shipley, C.; Arif, A. M.; Mitchell, M.; Halfen, J. A.; Berreau, L. M. *Inorg. Chem*. **2003**, *42*, 7472–7488. (g) He, Z.; Craig, D. C.; Colbran, S. B. *J. Chem. Soc., Dalton Trans*. **2002**, 4224–4235. (h) He, Z.; Colbran, S. B.; Craig, D. C. *Chem.—Eur. J*. **2003**, *9*, 116–129. (i) Mandon, D.; Machkour, A.; Goetz, S.; Welter, R. *Inorg. Chem*. **2002**, *41*, 5364–5372. (j) Mandon, D.; Nopper, A.; Litrol, T.; Goetz, S. *Inorg. Chem*. **2001**, *40*, 4803–4806.

sought to use $[M(\mathbf{2})]^{n+}$ complexes to build a hydrophobic cavity to accommodate other small molecules for the development of synthetic receptors and enzyme models such as for the active site of carbonic anhydrase, which contains a hydrophobic cavity above the $Zn^{2+}(His)_3$ moiety.[23] X-ray structures of Cu^{+} and Cu^{2+} complexes of **2** showed that such a hydrophobic cavity exists,[21i] but the poor solubility of **2** and its complexes prevented thermodynamic and kinetic studies. In the course of these studies, useful fluorescence properties were discovered that are the subject of this manuscript.

In this Article, substituted analogues of **2** are reported that render it soluble in most organic solvents (compound **3**) and in water (compound **4**). Solid-state structures of selected ligand and zinc complexes were determined by X-ray crystallography, and spectroscopic properties, such as NMR, UV absorbance, and fluorescence, were employed to deduce the relationships between the structures of the Zn^{2+}−ligand **3** complexes and the mechanisms of fluorescence enhancement associated with Zn^{2+} binding.

Experimental Section

All solvents and reagents were purchased from commercial sources and used as received. Solvents used for spectroscopic measurements were HPLC grade. UV−visible spectra were acquired on an Agilent 8453 UV−vis spectrometer. Circular dichroism spectra were recorded on an AVIV model 202SF spectropolarimeter. NMR spectra were obtained on Varian 300 MHz and Bruker AVANCE 400 MHz spectrometers. Mass spectra were recorded on an Omni Flex matrix-assisted laser desorption ionization-time-of-flight (MALDI-TOF) mass spectrometer or Thermo Finnigan PolarisQ gas chromatography−mass spectrometer (GC−MS). Melting points were taken in open tubes in a MelTemp II capillary melting point apparatus. Elemental analysis was performed by Quantitative Technologies, Inc. (Whitehouse, NJ). X-ray structures were determined at the X-ray crystallography laboratory, University of Minnesota (Minneapolis, MN).

Potentiometric Titrations. Potentiometric studies were conducted with a Titrino 702 autotitrator (Brinkmann Instruments). A Metrohm combined pH glass electrode (Ag/AgCl) with 3 M NaCl internal filling solution was used. All potentiometric titrations were carried out at a concentration of 4 mM, with $I = 0.10$ M $NaClO_4$, at 25 °C. The Zn^{2+} solution was standardized with primary standard EDTA in a NH_4OH/NH_4Cl buffer with EBT indicator. Standardizations of Cu^{2+} employed Fast-Sulphon black-F as an indicator, with the same buffer and EDTA standard. Ag^{+} and Pb^{2+} were used as prepared without any standardization. The NaOH solution was standardized against potassium hydrogen phthalate with phenolphthalein as an indicator. The $HClO_4$ solution was standardized with a standardized NaOH solution. Water was degassed by boiling for 1 h and then cooled under N_2. All solutions were carefully protected from air by a stream of N_2 gas. The k_w value was chosen as 13.78 for 25 °C, 0.10 M $Na(ClO_4)_2$. A Gran's plot using the NaOH solution found the carbonate content below the acceptable limit of 2%. Ligand concentration was determined gravimetrically using formulas determined by elemental analysis. A total of 3 equiv of $HClO_4$ was added to ligands in the absence of zinc to determine ligand protonation constants. The ligand−zinc binding constants and zinc-bound water acidity were determined in the presence of 1 equiv of Zn(II) ion from $Zn(ClO_4)_2$. About 100 data points were collected for each titration. The equilibrium constants were calculated using the program BEST-7. Sigma-fit values (as defined in the program) were smaller than 0.015. All constants were determined using at least two independent titrations.

X-ray Structure Determinations. A crystal of each sample was placed onto the tip of a 0.1 mm diameter glass capillary and mounted on a CCD area detector diffractometer for data collection at 173(2) K. A preliminary set of cell constants was calculated from reflections harvested from 3 sets of 20 frames or 4 sets of 50 frames. The data collection was carried out using Mo Kα radiation (graphite monochromator) with a frame time of 60 or 90 s and a detector distance of 4.9 cm. A randomly oriented region of reciprocal space was surveyed to the extent of one sphere and to a resolution of between 0.84 and 0.77 Å. Four major sections of frames were collected with 0.30° steps in ω at four different φ settings and a detector position of −28° in 2θ. The structures were solved using Bruker SHELXTL or SIR97 and refined using Bruker SHELXTL. The space groups were determined based on systematic absences and intensity statistics. Direct-method solutions were calculated which provided most non-hydrogen atoms from the E-map. Full-matrix least-squares/difference Fourier cycles were performed which located the remaining non-hydrogen atoms. All non-hydrogen atoms were refined with anisotropic displacement parameters. All hydrogen atoms were placed in ideal positions and refined as riding atoms with relative isotropic displacement parameters.

For $[Zn(\mathbf{3})(CH_3CN)](ClO_4)_2$, a preliminary set of cell constants was calculated from reflections harvested from 4 sets of 50 frames. This produced initial orientation matrixes determined from 488 reflections for two nonmerohedral twin component, these are related by a 180 deg rotation about [010] in reciprocal space.[24] Final cell constants were calculated from 2937 strong reflections from the actual data collection after the twin integration (SAINT).[25] The intensity data were corrected for absorption and decay (TWINABS).[26] Redundant reflections were removed from the final SHELX HKLF 5 data file with STRIP_REDUNDANT.[27] Structure solution and refinement was performed with SHELXTL, V6.12.[28] A rigid motion of one 3,4,5-trimethoxyphenyl group could not be refined and resulted in several persistent problems in the structure.

Fluorescence Lifetime Spectrometer. The fluorescence decay profiles were measured using the FluoTime single photon counting system (FluoTime 200) from PicoQuant Gmbh (Berlin, Germany) using a Hamamatsu H5783P photomultiplier tube. As a source of excitation, a femtosecond TiSp laser (Coherent MIRA 900) that is pumped with an argon ion laser (Coherent Innova 310) was utilized. The Mira 900 laser has pulse width of ~120 fs. In order to obtain the best resolution in our time domain of interest, the MIRA 900 output was passed through a Conoptics electrooptic light modulator system consisting of a model 350-160 modulator, a model 25D digital amplifier, and a M305 synchronous countdown device to reduce the laser pulse frequency from a repetition rate of 76 to 12 MHz. A Phillips Scientific wideband amplifier (model 6954) was used to amplify and normalize the synchronization pulses from the Mira 900 laser. The Mira 900 laser system has a wavelength output in the range of 700−1000 nm. A third harmonic generator was used to provide excitation in the UV part of the spectrum. An Aries FF250 monochromator was used in front of the photomultiplier tube to select the fluorescence emission wavelength of interest. We reduced the photon count rate to

(23) (a) Christianson, D. W.; Fierke, C. A. *Acc. Chem. Res.* **1997**, *29*, 331–339. (b) Marino, T.; Russo, N.; Toscano, M. *J. Am. Chem. Soc.* **2005**, *127*, 4242–4253. (c) Xu, J.; Chuang, C.-L.; Canary, J. W. *Inorg. Chim. Acta* **1997**, *256*, 125–128.

(24) Sheldrick, G. *CELL_NOW*, V1.03; 2003.

(25) *SAINT*, V6.35A; Bruker Analytical X-Ray Systems: Madison, WI, 2001.

(26) Sheldrick, G. *TWINABS*, V1.05, An empirical correction for absorption anisotropy: Blessing, R., *Acta Crystallogr.*, **1995**, *A51*, 33−38.

(27) Brennessel, W.; Young, V.G., Jr. *STRIP_REDUNDANT*, V1.3 (unpublished); 2004.

(28) *SHELXTL*, V6.12; Bruker Analytical X-Ray Systems: Madison, WI, 2000.

not more than 10 000 counts/s to obtain the best time resolution in our experiments. A Time Harp 100 PC card (PicoQuant, Germany) controlled by an IBM PC computer was used to control the experiments, to accumulate the photon counts, and to analyze the decay profiles by deconvolution methods with a time resolution of ~35 ps using the FluoFit software.

Tris-[6-(3,4,5-trimethoxy-phenyl)-pyridin-2-ylmethyl]-amine (3). A flask equipped with a reflux condenser, a septum inlet and a magnetic stirring bar was charged with **5** (46.2 mg, 0.2 mmol), 3,4,5-trimethoxyphenyl boronic acid (424 mg, 2.0 mmol), and $Pd(PPh_3)_4$ (140 mg, 0.04 mmol). The flask was flushed with argon gas and charged with toluene (1.5 mL), CH_3OH (1.0 mL), and aqueous Na_2CO_3 solution (2.0 M, 1.5 mL). The mixture was heated at 100 °C (bath temperature) with vigorous stirring for 16 h. The reaction was cooled, and the solvent was removed under vacuum. The residue was partitioned between ether (25 mL) and 5% HCl (50 mL). The organic layer was discarded, and the aqueous phase was washed with another portion of ether (25 mL). Subsequently, the aqueous phase was basified carefully with saturated Na_2CO_3 solution and extracted with methylene chloride (2 × 50 mL). The methylene chloride portions were combined and dried over Na_2SO_4. Dark residue resulted from the removal of solvent which was subjected to silica chromatography (methylene chloride/ethyl acetate = 3/1) to yield 133 mg of pure product (white solid, yield 84%). Melting point: 68−71 °C. ^{1}H NMR ($CDCl_3$, 400 MHz): δ = 7.77 (t, J = 7.4 Hz, 3H, Ar−H), 7.69 (d, J = 7.4 Hz, 3H, Ar−H), 7.60 (d, J = 7.5 Hz, 3H, Ar−H), 7.30 (s, 6H, Ar−H), 4.15 (s, 6H, CH_2), 3.98 (s, 18H, CH_3), 3.93 (s, 9H, CH_3). ^{13}C NMR ($CDCl_3$, 100 MHz): δ = 159.8, 156.4, 153.5, 139.0, 137.1, 135.2, 120.8, 118.5, 104.3, 60.9, 60.4, 56.2. ESI-MS: m/z 789.4 ($M + H^+$), 395.2 [($M + 2H^+$)/2]; calculated, 789.3, 395.2. Anal. Calcd (mass %) for $C_{45}H_{48}N_4O_9$: C, 68.51; H, 6.13; N, 7.10. Found: C, 68.12; H, 6.18; N, 6.79.

[Zn(3)(CH_3CN)](ClO_4)$_2$. (***Caution!*** *Perchlorate salts of metal complexes with organic ligands are potentially explosive. They should be handled in small quantities and with caution.*) The quantity 3.0 mL of 10 mM methanolic solution of **3** was mixed with 1.5 mL of 20 mM methanolic solution of $Zn(ClO_4)_2 \cdot 6CH_3CN$ (prepared by coevaporation of $Zn(ClO_4)_2 \cdot 6H_2O$ with dry acetonitrile) and allowed to sit without stirring for 3 days. Colorless crystals were collected and washed with methanol, and some single crystals were selected for crystallography. The yield was 51%. Melting point: 220−222 °C. ^{1}H NMR (CD_3CN, 400 MHz): δ = 8.25 (t, J = 7.8 Hz, 3H, Ar−H), 7.80 (d, J = 7.7 Hz, 3H, Ar−H), 7.69 (d, J = 7.9 Hz, 3H, Ar−H), 6.69 (s, b, 3H, Ar−H), 5.84 (s, b, 3H, Ar−H), 4.59 (s, 6H, CH_2), 3.90 (s, b, 9H, CH_3), 3.76 (s, 9H, CH_3), 3.11 (s, b, 9H, CH_3). Anal. Calcd (mass %) for $C_{45}H_{48}Cl_2N_4O_{17}Zn \cdot CH_3CN \cdot H_2O$: C, 50.75; H, 4.80; N, 6.30. Found: C, 50.62; H, 4.64; N, 6.19.

Cu(3)(ClO_4)$_2$. (***Caution!*** *Perchlorate salts of metal complexes with organic ligands are potentially explosive. They should be handled in small quantities and with caution.*) The quantity 2.0 mL of 10 mM methanolic solution of **3** was mixed with 0.2 mL of 100 mM methanolic solution of $Cu(ClO_4)_2 \cdot 6H_2O$. Green crystals formed after 10 min with a yield of 74%. Melting point: 190−194 °C. Anal. Calcd (mass %) for $C_{45}H_{48}Cl_2CuN_4O_{17} \cdot H_2O$: C, 50.54; H, 4.71; N, 5.24. Found: C, 50.57; H, 4.56; N, 5.27.

5-Iodobenzene-1,2,3-triol (7). 5-Iodo-1,2,3-trimethoxybenzene (**6**) (5.0 g, 17.0 mmol) and trimethylsilyl iodide (20.4 g, 102 mmol) was mixed in 50 mL of dry acetonitrile and refluxed for 72 h. The solution was poured into 20 mL of methanol to quench the reaction after cooling to ambient temperature. Solvents were removed, and the residue was partitioned between 200 mL of ether and 50 mL of 1 M HCl solution. The ether layer was washed twice with 50 mL of 1 M sodium thiosulfate and once with 50 mL of brine. A quantity of 4.05 g of white powder product was produced after the organic layer was dried by anhydrous $MgSO_4$ and condensed under vacuum. The yield was 95%. Melting point: 132−134 °C. ^{1}H NMR (acetone-d_6, 300 MHz): δ = 8.20 (s, 2H, OH), 7.56 (s, 1H, OH), 6.73 (s, 2H, Ar−H). ^{13}C NMR (acetone-d_6, 75.5 MHz): δ = 148.9, 135.3, 118.5, 81.3.

1,2,3-Tris(2-(2-(2-methoxyethoxy)ethoxy)ethoxy)-5-iodobenzene (8). Compound **7** (2.97 g, 11.8 mmol) and anhydrous potassium carbonate (19.6 g, 142 mmol) were mixed in 60 mL of dry DMF and stirred at 100 °C for 20 min. Then 2-(2-(2-methoxyethoxy)ethoxy)ethyl 4-methylbenzenesulfonate (ROTs)[29] (15.0 g, 47.2 mmol) was added slowly and stirring was continued at 100 °C for 20 h. The solvent was removed, and the residue was subjected to extraction between ethyl acetate (300 mL) and water (5 × 50 mL). The organic solution was dried with anhydrous sodium sulfate and the solvent was removed. A silica gel column eluted with 40:1 methylene chloride/methanol was used to purify the product, affording 6.45 g of light yellow oil (yield 79%). ^{1}H NMR ($CDCl_3$, 300 MHz): δ = 6.91 (s, 2H, Ar−H), 4.15−4.08 (m, 6H, CH_2), 3.88−3.50 (m, 30H, CH_2), 3.38 (s, 9H, CH_3). ^{13}C NMR ($CDCl_3$, 50 MHz): δ = 153.8, 118.0, 86.3, 72.8, 72.5, 71.4, 71.2, 71.1, 71.1, 70.2, 69.7, 59.6. MALDI-TOF MS: m/z 713.3 ($M + Na^+$); calculated, 713.2. Anal. Calcd (mass %) for $C_{27}H_{47}IO_{12}$: C, 46.96; H, 6.86. Found: C, 47.01; H, 6.71.

3,3,4,4-Tetramethyl-1-(3,4,5-tris(2-(2-(2-methoxyethoxy)-ethoxy)ethoxy)phenyl)-borolane (9). Compound **8** (2.90 g, 4.2 mmol) and $PdCl_2(dppf) \cdot CH_2Cl_2$ (106 g, 0.13 mmol, 3%) were mixed in 15 mL of dry 1,4-dioxane. Dry triethylamine (1.28 g, 12.6 mmol) and pinacolborane (1.08 g, 8.4 mmol) were added dropwise sequentially under an argon atmosphere. The solution was heated at 80 °C for 2 h, and the solvent was removed after cooling. Ether (300 mL) and water (3 × 100 mL) were used for extractive isolation. The organic solution was dried with sodium sulfate and the ether was evaporated. Alumina chromatography eluted with 2:1 methylene chloride/ethyl acetate gave 1.86 g of reddish oil product (yield: 64%). ^{1}H NMR ($CDCl_3$, 200 MHz): δ = 7.00 (s, 2H, Ar−H), 4.21−4.11 (m, 6H, CH_2), 3.88−3.48 (m, 30H, CH_2), 3.36 (s, 9H, CH_3), 1.31 (s, 12H, CH_3). ^{13}C NMR ($CDCl_3$, 50 MHz): δ = 152.7, 141.6, 114.1, 84.3, 72.8, 72.5, 71.3, 71.2, 71.0, 70.3, 69.2, 59.6, 25,5. MALDI-TOF MS: m/z 712.8 ($M + Na^+$); calculated, 713.4. Anal. Calcd (mass %) for $C_{33}H_{59}BO_{14}$: C, 57.39; H, 8.61. Found: C, 57.36; H, 8.51.

Tris((6-(3,4,5-tris(2-(2-(2-methoxyethoxy)ethoxy)ethoxy)-phenyl)pyridin-2-yl)-methyl)amine (4). The compounds **9** (1.45 g, 2.10 mmol), **5** (138 mg, 0.262 mmol), and $Pd(PPh_3)_4$ (61 mg, 0.053 mmol, 20%) were added to a solution composed of 2 mL of toluene, 1.4 mL of methanol, and 2 mL of 2 M Na_2CO_3 and stirred at 100 °C for 20 h under argon. After the mixture was cooled and the solvent was removed, 50 mL of ether and 100 mL of 6 M HCl were added for extraction. The aqueous layer was washed with 50 mL of methylene chloride and basified with saturated sodium hydroxide carefully until the pH reached 10. This aqueous solution was washed twice with 100 mL of methylene chloride, and the combined organic layer was dried with sodium sulfate. Silica gel chromatography with 30:1 methylene chloride/MeOH produced 298 mg of light yellow oil product (yield: 69%). ^{1}H NMR ($CDCl_3$, 300 MHz): δ = 7.74−7.62 (m, 6H, Ar−H), 7.50 (d, 3H, J = 7.4 Hz, Ar−H), 7.27 (s, 6H, Ar−H), 4.23 (t, 12H, J = 5.0 Hz, CH_2), 4.18 (t, 6H, J = 5.2 Hz, CH_2), 4.02 (s, 6H, CH_2), 3.86 (t, 12H, J = 5.0 Hz, CH_2), 3.80 (t, 6H, J = 5.1 Hz, CH_2), 3.76−3.71 (m, 18H, CH_2), 3.68−3.60 (m, 36H, CH_2), 3.56−3.50 (m, 18H, CH_2), 3.36 (s, 9H, CH_3), 3.35 (s, 18H, CH_3). ^{13}C NMR ($CDCl_3$, 75.5 MHz): δ = 160.8, 157.1, 154.0, 141.4, 137.8, 136.0, 122.0, 119.1, 108.9, 73.5, 73.1, 71.9, 71.8, 71.6, 71.0, 70.5, 61.7, 59.8. MALDI-TOF MS: m/z 1979.4 ($M + H^+$); calculated, 1979.1. Anal. Calcd

(29) Selve, C.; Ravey, J.-C.; Stebe, M.-J.; El Moudjahid, C.; Moumni, E. M.; Delpuech, J.-J. *Tetrahedron* **1991**, *47*, 411–428.

Scheme 1. Syntheses of Triphenyl Substituted TPA Compounds[a]

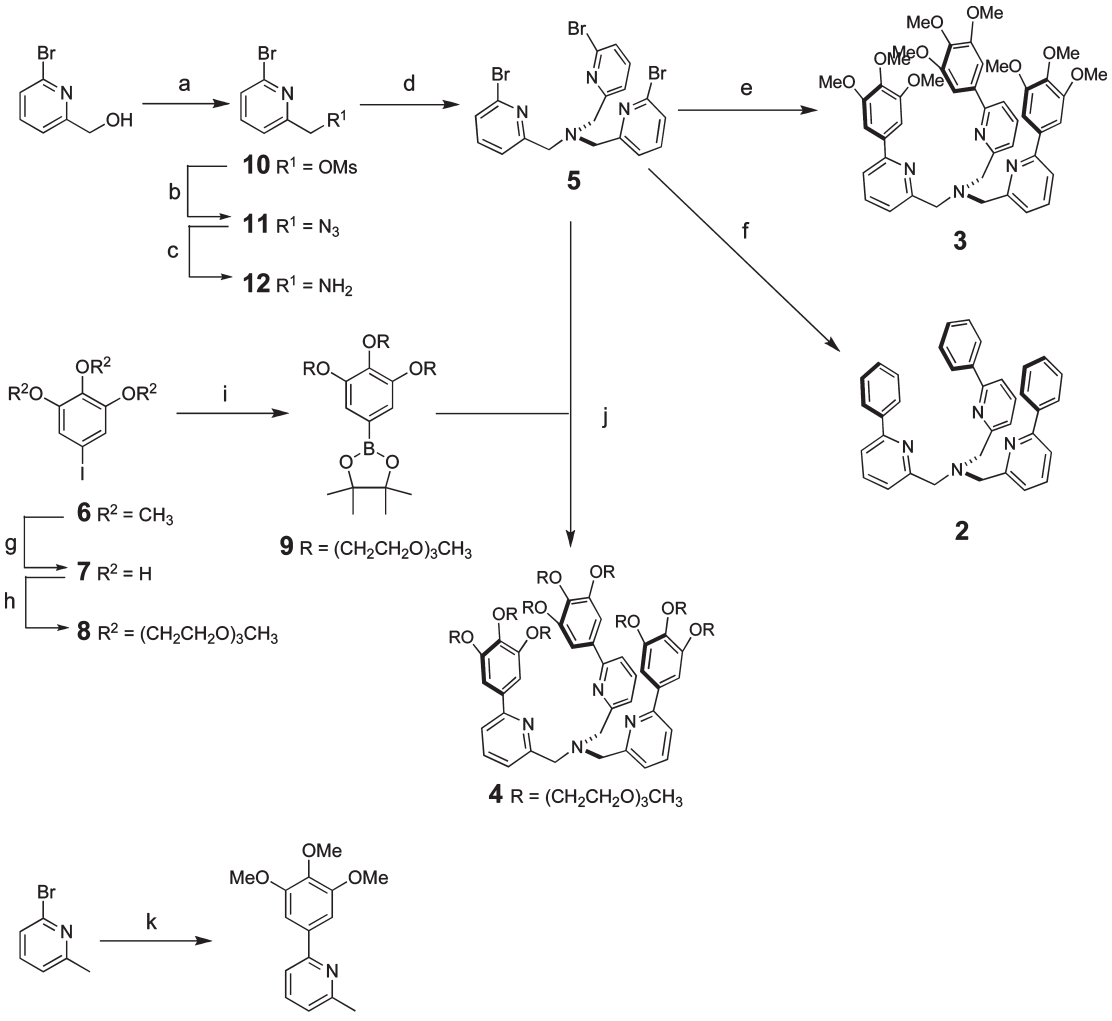

[a] Conditions: (a), MsCl, TEA, CH_2Cl_2, 98%; (b), NaN_3, 18-crown-6, CH_3CN, 87%; (c), PPh_3, THF, H_2O, 72%; (d), **10**, K_2CO_3, DMF, 81%; (e), 3,4,5-trimethoxyphenyl boronic acid, $Pd(PPh_3)_4$, Na_2CO_3, toluene, MeOH, H_2O, 84%; (f), phenyl boronic acid, $Pd(PPh_3)_4$, $Ba(OH)_2$, DME, H_2O, 80%; (g), Me_3SiI, CH_3CN, MeOH, 95%; (h), $CH_3(OCH_2CH_2)OTs$, K_2CO_3, DMF, 79%; (i), $PdCl_2(dppf)\cdot CH_2Cl_2$, pinacolborane, TEA, dioxane, 64%; (j), **9**, $Pd(PPh_3)_4$, Na_2CO_3, toluene, MeOH, H_2O, 69%; (k), 4,5-trimethoxyphenyl boronic acid, $Pd(PPh_3)_4$, Na_2CO_3, toluene, MeOH, H_2O, 91%.

(mass %) for $C_{99}H_{156}N_4O_{36}$: C, 60.11; H, 7.95; N, 2.83. Found: C, 59.94; H, 7.94; N, 2.90.

2-Methyl-6-(3,4,5-trimethoxy-phenyl)-pyridine (13). 6-Bromo-2-methylpyridine (151 mg, 0.88 mmol) was reacted with 3,4,5-trimethoxyphenyl boronic acid (212 mg, 1.0 mmol) with the same reaction conditions and workup procedure as described for the preparation of **3**. Silica gel chromatography with 1:2 methylene chloride/ethyl acetate yielded 208 mg of light yellow oil. The yield was 91%. ^{1}H NMR ($CDCl_3$, 300 MHz): δ (ppm): 7.63 (t, J = 7.7 Hz, 1H, Ar−H), 7.46 (d, J = 7.7 Hz, 1H, Ar−H), 7.20 (s, 2H, Ar−H), 7.09 (d, 1H, J = 7.5 Hz, Ar−H), 3.96 (s, 6H, CH_3), 3.89 (s, 3H, CH_3), 2.63 (s, 3H, CH_3). ^{13}C NMR ($CDCl_3$, 75.5 MHz): δ (ppm): 159.3, 157.7 154.7, 137.6, 136.4, 122.2, 118.0, 106.6, 61.7, 57.5, 25.5. ESI-MS: m/z 260.1 ($M + H^+$); calculated, 260.3. Anal. Calcd (mass %) for $C_{15}H_{17}NO_3$: C, 69.48; H, 6.61; N, 5.40. Found: C, 69.20; H, 6.53; N, 5.17.

Results and Discussion

Synthesis. Compound Br_3TPA (**5**, Scheme 1) served as a scaffold to build tris((6-phenyl-2-pyridyl)methyl)amine (**2**) and its soluble derivatives (**3**, **4**). The three bromine substituents can be derivatized with phenyl boronic acids or esters by Suzuki coupling.[30] The preparation of **5** was reported previously.[21g] However, in the present work, a modified procedure afforded better overall yield. Alcohol (6-bromo-2-pyridyl)methanol was reacted with mesyl chloride to give **10**[31] and then converted to an azide (**11**), which was subsequently reduced to a primary amine (**12**). Finally, compound **12** was alkylated with the mesylate **10** in a 1:2 ratio to afford **5**. Each step in this sequence gave good yield (overall 49%), and chromatographic separation was not required until the last step. Thereafter, ligands **2** and **3** were prepared via Suzuki coupling between tribromo-substituted compound **5** and the

(30) (a) Malleron, J.-L.; Fiaud, J.-C.; Legros, J.-Y. *Handbook of Palladium-Catalyzed Organic Reactions: Synthetic Aspects and Catalytic Cycles*; Academia Press: San Diego, CA, 1997. (b) Tsuji, J.; *Palladium Reagents and Catalysts: Innovations in Organic Synthesis*; Wiley & Sons: Chichester, U.K., 1995.(c) Miyaura, N.; Suzuki, A. *J. Organomet. Chem.* **1981**, *213*, C53–C56.

(31) The alcohol is commercially available, but it can also be made from 2,6-dibromopyridine by reacting with BuLi, DMF, and $NaBH_4$ subsequently. The mesylation of this alcohol was reported when we did the reaction under the same condition: Puglisi, A.; Benaglia, M.; Roncan, G. *Eur. J. Org. Chem.* **2003**, 1552–1558.

Table 1. Summary of Crystal Data and Structure Refinement for [Zn(**2**)(CH_3CN)](ClO_4)$_2$, [Zn(**3**)(CH_3CN)](ClO_4)$_2$, **3**, and [H(**3**)]ClO_4

	[Zn(**2**)(CH_3CN)] (ClO_4)$_2$	[Zn(**3**)(CH_3CN)] (ClO_4)$_2$	**3**	[H(**3**)]ClO_4
formula	$C_{38}H_{33}Cl_2N_5O_8Zn$	$C_{95}H_{108}Cl_4N_{10}O_{36}Zn_2$	$C_{45}H_{47}N_4O_9$	$C_{45}H_{49}ClN_4O_{13}$
M_T	823.96	2238.45	787.87	889.33
T (K)	173(2)	173(2)	173(2)	173(2)
λ (Å)	0.71073	0.71073	0.71073	0.71073
space group	$P\bar{1}$	$P\bar{1}$	$P2_1/c$	$P2_1/n$
a (Å)	10.964(2)	11.013(3)	31.378(5)	13.7244(16)
b (Å)	13.374(3)	19.492(6)	10.0581(15)	11.3897(13)
c (Å)	13.472(3)	23.662(7)	12.9625(19)	27.094(3)
α (deg)	91.340(4)	93.129(6)	90	90
β (deg)	111.942(4)	102.854(5)	100.347(3)	95.030(2)
γ (deg)	94.282(4)	91.217(6)	90	90
V (Å^3)	1824.4(7)	4942(3)	4024.5(10)	4219.0(8)
Z	2	2	4	4
ρ (mg/m^3)	1.500	1.505	1.300	1.400
μ (mm^{-1})	0.880	0.686	0.091	0.164
final R indices [$\lambda > 2\sigma(\lambda)$][a]	$R_1 = 0.0378$, wR2 = 0.0951	$R_1 = 0.0723$, wR2 = 0.1742	$R_1 = 0.0565$, wR2 = 0.1189	$R_1 = 0.0686$, wR2 = 0.1799
R indices (all data)	$R_1 = 0.0505$, wR2 = 0.1014	$R_1 = 0.0873$, wR2 = 0.1815	$R_1 = 0.1192$, wR2 = 0.1450	$R_1 = 0.1009$, wR2 = 0.2017

[a] $R_1 = \Sigma||F_o| - |F_c||/\Sigma|F_o|$; wR2 = $[\Sigma[w(F_o^2 - F_c^2)^2]/\Sigma[w(F_o^2)^2]]^{1/2}$, where $w = q/[\sigma^2(F_o^2) + (aP)^2 + bP + d + e\sin(\theta)]$

appropriate boronic acids. The synthesis of compound **2** by another route was reported previously.[21i]

Compound **4** was prepared by a convergent approach. Iodobenzenetriol (**7**) was first obtained from demethylation of iodotrimethoxybenzene (**6**). Ethylene glycol groups were then added to **7** to afford polyether **8**. Compound **8** was subsequently converted to boronic ester **9** and then coupled with **5** to afford the final compound **4**. The purity of the final compound **4** was satisfactory, as evidenced by NMR and elemental analysis. Boronic ester **9** is a useful water-soluble building block that may be used with other molecular scaffolds, but one should note that it is sensitive to silica gel. Therefore, alumina chromatography is required for its purification.

Solubility comparisons of ligands **1**−**4** indicate that, although TPA (**1**) is very soluble in organic solvent as well as in water, the triphenyl substituted compound (**2**) is barely soluble in most solvents. Compound **3** has nine methoxyl groups on the rims of the phenyl substituents, adding more aliphatic carbons and heteroatoms, which results in reasonable solubility in most polar organic solvents. Incorporation of ethylene glycol moieties tends to improve aqueous solubility of organic compounds.[32] Compound **4** was prepared with nine incorporated triethylene glycol groups and subsequently found to dissolve easily in water (> 70 mg/mL).

Solid State Structures. Crystals of the complex [Zn(**2**)(CH_3CN)](ClO_4)$_2$ were obtained by diffusing THF into a CH_3CN solution of ligand **2** and 1 equiv of $Zn(ClO_4)_2$. The crystal structure was determined by X-ray crystallography, and the relevant data collection and refinement parameters are shown in Table 1. As shown in Figure 1A, the zinc atom adopts a distorted trigonal bipyramidal configuration, which is very similar to the structures of [Zn(**1**)Cl]ClO_4[33a] and [Cu(**2**)(CH_3CN)](ClO_4)$_2$.[21i] The three arms of the ligand surround the metal ion to form a hydrophobic cavity defined by the phenylpyridyl groups, encasing a CH_3CN ligand. The distances between Zn and N vary from 2.04 to 2.16 Å. The depth of the cavity (as defined by the distance from the zinc atom to the center of three most remote carbons on the arms) is 3.8 Å, slightly shorter than the distance between zinc and the remote carbon of the acetonitrile molecule (4.6 Å). The dihedral angles between the phenyl substituents and pyridyl groups range from 37° to 45°, which put the phenyl substituents in close van der Waals contact with the CH_3CN ligand. The distances between the three aromatic nitrogen atoms (N2, N3, and N4) are 3.53, 3.55, and 3.56 Å, indicating that the three aromatic arms are folded up and close to each other. The distances from the remote carbon of the acetonitrile molecule to the closest carbon in each of the three phenyl groups are 3.62, 3.66, and 3.68 Å, in the range of van der Waals interactions.

Single crystals of [Zn(**3**)(CH_3CN)](ClO_4)$_2$ were obtained from in situ complexation of $Zn(ClO_4)_2 \cdot 6CH_3CN$ with **3** at a 1:1 ratio in methanol. There are two species in the crystal lattice. Their structures are almost identical except for the relative positions of the methoxyl groups; therefore, only one species is shown in Figure 1B. The zinc center adopts a distorted trigonal bipyramidal geometry, similar to that of [Zn(**2**)(CH_3CN)](ClO_4)$_2$. All four nitrogen atoms of the ligand and an acetonitrile molecule coordinate with the zinc ion. The two axial coordination positions are occupied by the tertiary nitrogen atom (N1b) and the acetonitrile nitrogen (N5b). All three arms form a compact hydrophobic cleft above the zinc ion, which is filled by the acetonitrile molecule. This structure is similar to that of [Zn(**2**)(CH_3CN)](ClO_4)$_2$ except for the nine additional methoxyl groups. The distances between the Zn and nitrogen atoms vary from 2.04 to 2.16 Å. The depth of the cavity (defined by the distance from the Zn atom to the center of three oxygens in the center top of the arms) is 4.7 Å, slightly longer than that of [Zn(**2**)-(CH_3CN)](ClO_4)$_2$. The dihedral angles between the phenyl substituents and the pyridyl groups range from 60° to 71°. Thus, the propeller-like twist of this complex is much larger than that of [Zn(**2**)(CH_3CN)](ClO_4)$_2$, bringing the

(32) Zeng, F.; Zimmerman, S. C. *Chem. Rev.* **1997**, *97*, 1681–1712.
(33) (a) Allen, C. S.; Chuang, C.-L.; Cornebise, M.; Canary, J. W. *Inorg. Chim. Acta* **1995**, *239*, 29–37. (b) Bretonnière, Y.; Mazzanti, M.; Pécaut, J.; Dunand, F. A.; Merbach, A. E. *Inorg. Chem.* **2001**, *40*, 6737–6745. (c) Zeng, X.; Coquière, D.; Alenda, A.; Garrier, E.; Prangé, T.; Li, Y.; Reinaud, O.; Jabin, I. *Chem.—Eur. J.* **2006**, *12*, 6393–6402.

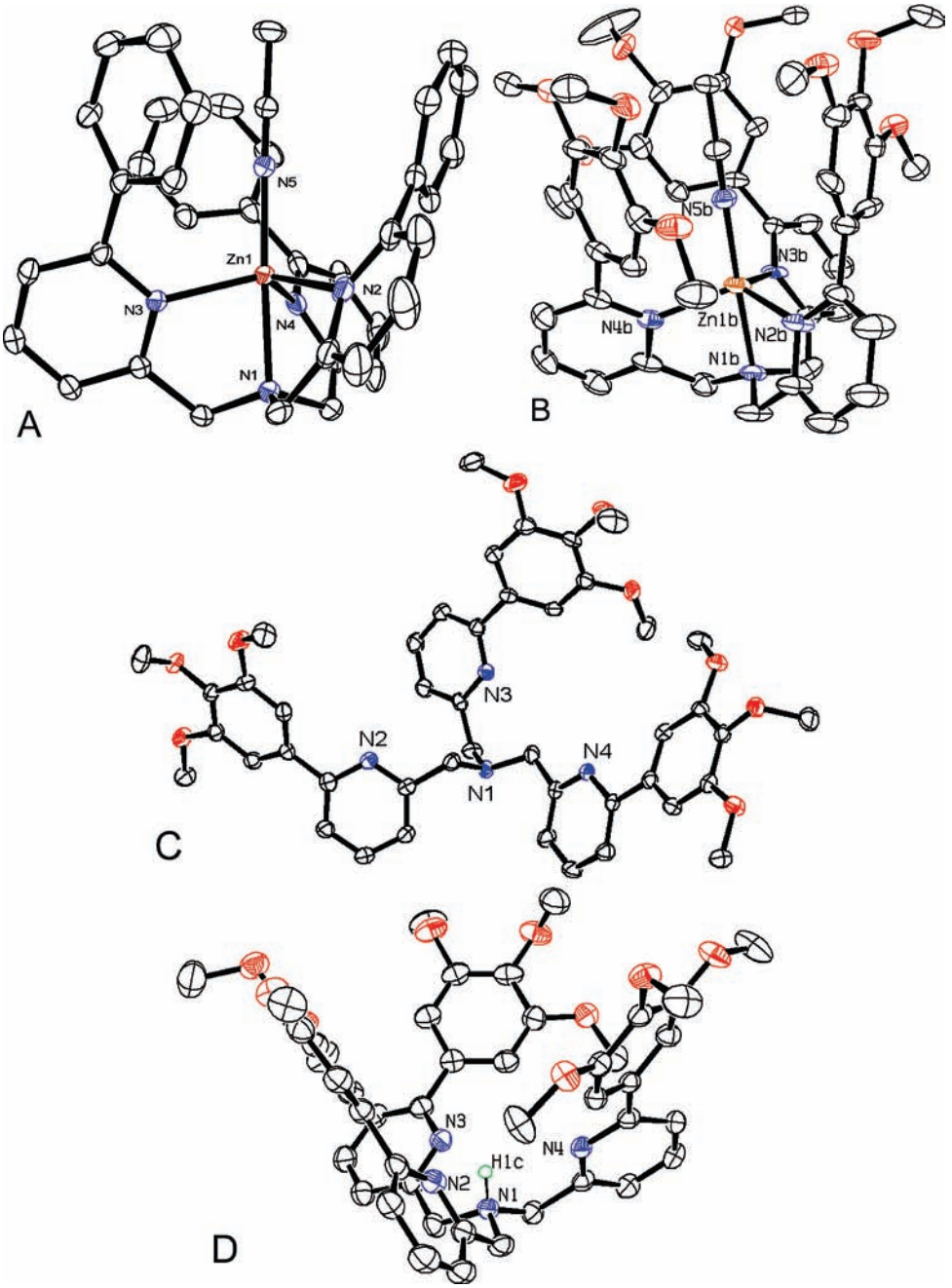

Figure 1. ORTEP diagrams (50% probability ellipsoids) of (A) [Zn(**2**)(CH_3CN)](ClO_4)$_2$; (B) [Zn(**3**)(CH_3CN)](ClO_4)$_2$; (C) free ligand **3**; and (D) protonated ligand [H(**3**)]ClO_4. Most hydrogen atoms and perchlorate counterions are omitted for clarity.

phenyl groups closer to the zinc ion. The distances between the three aromatic nitrogen atoms (N2b, N3b, and N4b) are 3.50, 3.59, and 3.64 Å, similar to that of [Zn(**2**)(CH_3CN)](ClO_4)$_2$. The distances from the top carbon of the acetonitrile molecule to the closest carbon in each of the three phenyl groups are 3.27, 3.27, and 3.34 Å, which are smaller than observed in [Zn(**2**)(CH_3CN)](ClO_4)$_2$. These shorter distances originate from the larger dihedral angles between the phenyl substituents and pyridyl groups.

In an attempt to prepare a Zn(II) complex by mixing ligand **3** and $Zn(ClO_4)_2 \cdot (H_2O)_6$ in a 2:1 ratio in methanol, crystals of ligand **3** and its $HClO_4$ salt were obtained instead, with the proton apparently originating from Zn^{2+}(aq). The sample presented ligand **3** crystals in two different protonated forms, the free base (Figure 1C) and the protonated ligand (Figure 1D). The two structures differ in that lone pair electrons of the tertiary nitrogen in the free base ligand point away from the three pyridine moieties, while in the $HClO_4$ salt the lone pair is protonated and oriented toward the nitrogen atom of the pyridyl groups. In the free base (Figure 1C), the dihedral angles between the phenyl substituents and pyridyl groups range from 17° to 34°. The distances between the three aromatic nitrogen atoms (N2, N3, and N4) are 4.55, 5.06, and 6.40 Å, respectively, which are much larger than those of the zinc complex. The $HClO_4$ salt has a folded structure (Figure 1D), much like what is observed in the zinc complex. The dihedral angles between the phenyl substituents and pyridyl groups range from 25° to 29°, which are close to the free ligand, however smaller

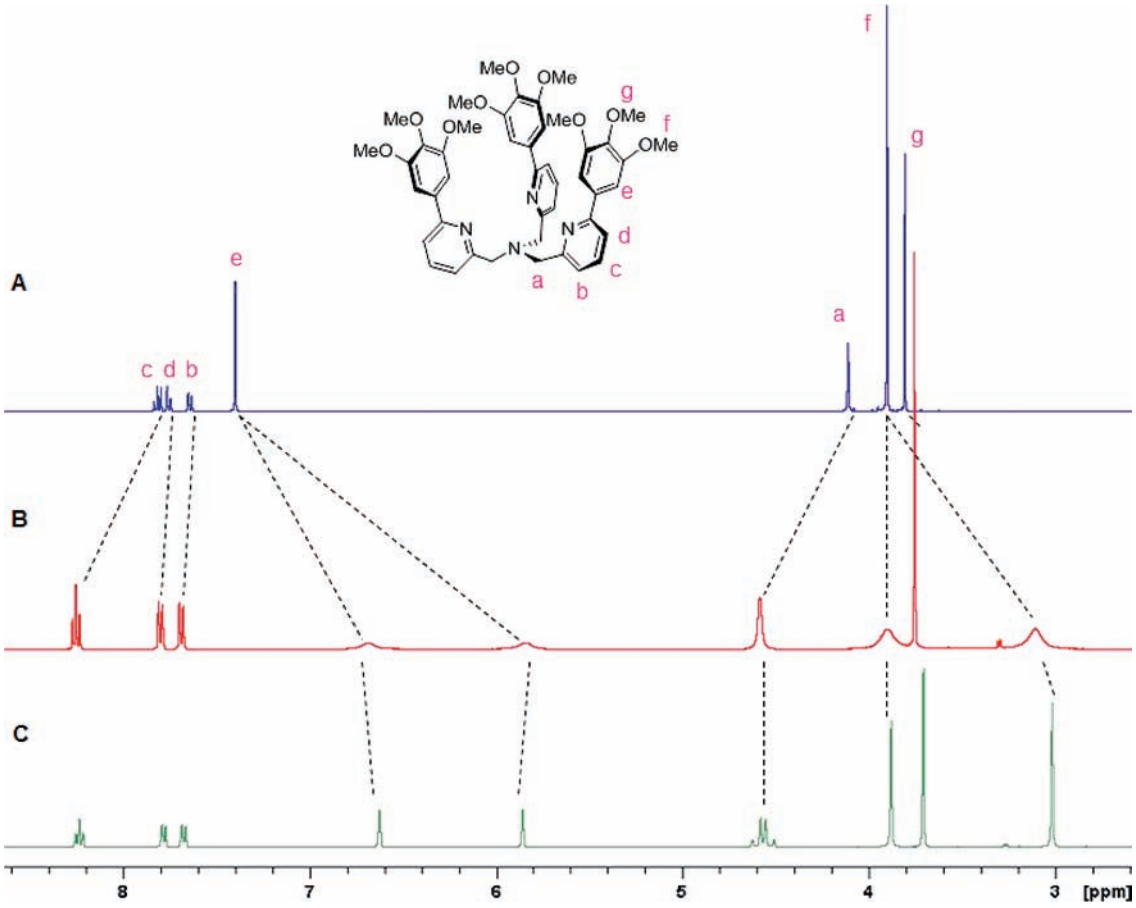

Figure 2. ^{1}H NMR spectra obtained in CD_3CN: (A) **3** at 25 °C; (B) $[Zn(\mathbf{3})]^{2+}$ at 25 °C; (C) $[Zn(\mathbf{3})]^{2+}$ at −10 °C.

than the zinc complex. The distances between the proton on the tertiary nitrogen atom (N1) and the three aromatic nitrogen atoms (N2, N3, and N4) are 2.37, 2.38, and 2.51 Å, respectively, and consistent with reported structures of similar protonated derivatives of TPA.[33b,c] The distances between the three aromatic nitrogen atoms (N2, N3, and N4) are 4.01, 4.12, and 4.28 Å, which are between those of the free ligand and the zinc complex. The overall features of the protonated ligand are similar to the zinc complex, but the protonated ligand conformation is more highly twisted to bring the pyridyl nitrogen atoms closer together to interact with the proton (H1c in Figure 1D).

NMR Characteristics. The ^{1}H NMR spectra of ligand **3** and its complex with zinc (Zn(**3**)) in CD_3CN are depicted in Figure 2. The binding properties of compound **3** with Zn^{2+} were also studied at different ratios of $Zn(ClO_4)_2$/ligand (Figure S4 in the Supporting Information).

The ^{1}H NMR spectrum of the free ligand **3** is shown in Figure 2A. The aromatic proton resonances b, c, and d are easily distinguishable by their multiplet structures. Proton e of the substituted phenyl ring is a singlet suggesting free rotation about the trimethoxyphenyl−pyridyl bond. There are two groups of Ar−OCH_3 methyl group proton resonances characterizing the central 4-methoxy- and the magnetically equivalent 3- and 5-methoxy protons.

The addition of $Zn(ClO_4)_2$ gives rise to some pronounced changes in the ^{1}H NMR spectrum of ligand **3** (Figure 2B and Figure S4 in the Supporting Information). With comparison of the ligand **3** and the Zn(**3**) NMR spectra, there is a shift and broadening of the methylene proton resonances a in the complex, while the single resonance of the 3- and 5-phenyl-methoxyl groups at 3.89 ppm in the ligand **3** (f) splits into two broadened resonances at 3.11 and 3.90 ppm in the Zn(**3**) complex (Figure 2B). However, the proton resonance of the central 4-methoxyl group remains sharp but is shifted slightly upfield in the zinc complex. These results indicate that the free rotation of the three aromatic arms is sterically hindered and that the protons of the 3- and 5-methoxyl groups are placed in different magnetic environments, while the protons of the 4-methoxyl group remain in a single magnetic environment in the Zn(**3**) complex. These resonances are sharpened when the temperature is lowered to −10 °C (Figure 2C). The splitting of resonances e and f is likely to result from a barrier to conformational exchange between right- and left-twisted ligand conformations that would exchange the protons attached to the methylene groups.[34] Figure S4 in the Supporting Information shows the titration of free ligand with aliquots of zinc salt. The addition of metal ions diminishes the resonance of the free ligand gradually while increasing that of the zinc complex until saturation is observed at 1 equiv of $Zn(ClO_4)_2$. The simultaneous observation of metal ion-coordinated complexes and free

(34) (a) Canary, J. W.; Allen, C. S.; Castagnetto, J. M.; Chiu, Y. H.; Toscano, P. J.; Wang, Y. H. *Inorg. Chem.* **1998**, *37*, 6255–6262. (b) Canary, J. W.; Zahn, S. *Trends Biotechnol.* **2001**, *19*, 251–255. (c) Holmes, A. E.; Simpson, S. A.; Canary, J. W. *Monatsh. Chem.* **2005**, *136*, 461–475.

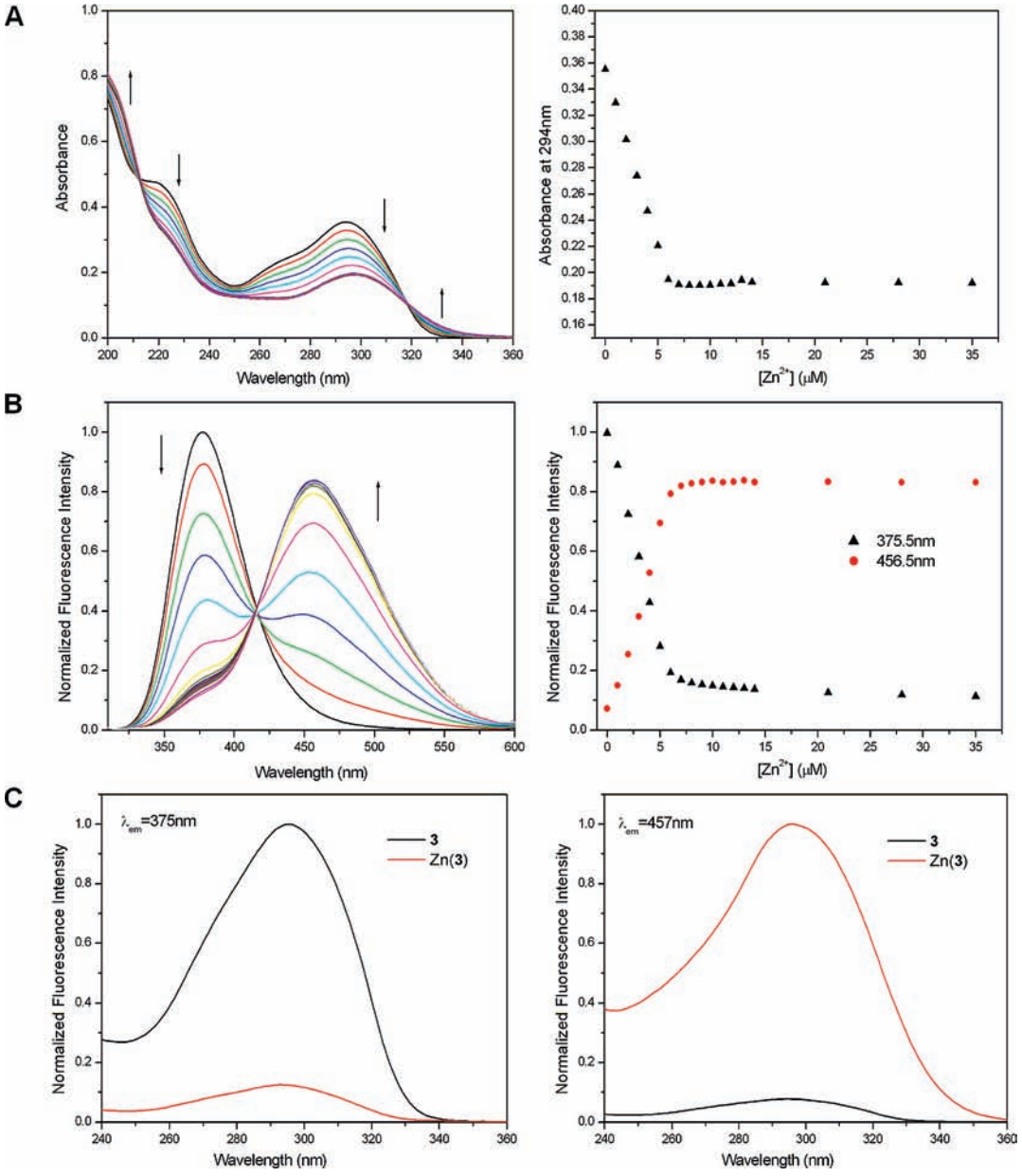

Figure 3. (A) UV titration of **3** with $Zn(ClO_4)_2$ in CH_3CN; (B) fluorescence titration of **3** with $Zn(ClO_4)_2$ in CH_3CN, the excitation wavelength is 300 nm; (C) excitation spectra of **3** and its zinc complex in CH_3CN, the emission wavelengths are 375 and 457 nm, respectively. In the UV and fluorescence titration, the concentration of ligand **3** is 7 μM and the lines represent the addition of 0, 1, 2, 3, 4, 5, 6, 7, 8, 9, 10, 11, 12, 13, 14, 21, 28, and 35 μM Zn^{2+}.

ligand spectra indicate that the rates of dissociation of Zn complexes are slower than the NMR time scale.

Spectroscopic Characteristics of Binding of Zn^{2+} to Ligands 3 and 4. We investigated the binding of Zn^{2+} to the water-insoluble ligand **3** in acetonitrile and to the water-soluble ligand **4** in aqueous solution.

Zn(3) Complexes. The UV absorbance and fluorescence characteristics of ligand **3** in the absence of Zn^{2+} and at different concentrations of Zn^{2+} ions in acetonitrile are summarized in Figure 3. The absorption spectrum exhibits a spectral broadening, a pronounced hypochromic effect, and a small red shift as the Zn^{2+} ion concentration is increased from 0 to 7 μM (panel A). The fluorescence emission spectrum of **3** exhibits a maximum at 376 that gradually shifts to 457 nm as the Zn^{2+} ion concentration is increased in the same range (panel B). The fluorescence intensity is enhanced by a factor of ~10 when measured at the 457 nm emission maximum, and a factor of > 100 when measured at 520 nm. The fluorescence excitation spectra of ligand **3** and the Zn^{2+}−ligand **3** complex, Zn(**3**), are similar in shape (panel C) like the UV absorption spectra (panel A). The red-shifted 457 nm fluorescence band of Zn(**3**) complexes gradually diminishes while the intensity at 376 nm increases as small amounts of water are added stepwise (Figure S10 in the Supporting Information). The 457 nm fluorescence band disappears completely at a 5% concentration of water indicating the complete conversion of the Zn(**3**) complex to the free ligand **3** has occurred at this concentration of water in acetonitrile.

The affinity of Zn^{2+} for compound **3** is much lower than that for TPA (**1**). It is well-known that TPA (**1**) is a strong binder of divalent metal ions, with binding constants of 10^{11} M^{-1} for Zn^{2+} and 10^{16} M^{-1} for Cu^{2+} in

aqueous solutions.[35] Analysis of the fluorescence titration data suggests that the binding constant of **3** with Zn^{2+} is about 10^8 M^{-1} in CH_3CN. Usually, the ligand−metal ion affinity should be higher in organic solvents than in aqueous media. This difference is likely a result of both steric and electronic effects of the phenyl substituent groups.[21h] The influence of steric effects is evident from the comparison of pyridine vs 2-methylpyridine, where the presence of a methyl group in the latter diminishes the binding constant, K, for complexation with Cu^{2+} from log K = 2.54 to 1.3, even though the electron donating methyl group makes the pyridine more basic (pK_a changes from 5.33 to 6.06). In comparison of pyridine with 2-phenylpyridine, the phenyl group makes pyridine both less basic (pK_a changes from 5.33 to 4.77) and a weaker ligand for binding with Cu^{2+} (log K changes from 2.54 to 1.3).[36] For TPA (**1**) vs tris((6-methylpyridyl)methyl)amine, it is known that the methyl groups on each of the three pyridine moieties in the latter compound cause the binding constant to drop from 16.15 to 10.52 for Cu^{2+} and from 11.00 to 5.45 for Zn^{2+} even though the pK_a increases from 6.2 to 6.9.[37] Thus, both steric factors and electronic factors can play significant roles in modulating the affinity of binding of Zn^{2+} and Cu^{+} ions.

Zn(4) Complexes. The triethylene glycol substituted compound **4** was found to be soluble in water. The protonation constants (K_1, K_2, and K_3) were determined by potentiometric titration of ligand·$3H^+$ using 0.1 M NaOH at 25 °C with I = 0.1 M (Figure S5 in the Supporting Information). As determined by the BEST-7 program, with a σ value of 0.81%,[38] log K_1 was found to be 7.29. K_2 and K_3 were $<$2.5 and therefore did not give a transition in aqueous solution. The increased basicity of compound **4** compared to the log K_1 of TPA (6.17),[35] **4** testifies to the strong effect of the three electron-releasing alkoxyl substitutents to reverse the electronic effect normally observed for phenyl groups attached to the 6-position of pyridines.

No evidence could be obtained for the complexation of **4** with metal ions in aqueous solution. The determination of the zinc−ligand binding constant and zinc-bound water acidity was also attempted with potentiometric titrations of ligand·$3H^+$ in the presence of 1 equiv of $Zn(ClO_4)_2$, but only precipitation of $Zn(OH)_2$ was observed. Similar results were obtained with Cu^{2+}, Pb^{2+}, and Ag^+ salts.[35] ^{1}H NMR, UV−vis, and fluorescence measurements did not provide any evidence for complexation of **4** in water. Comparison of ^{1}H NMR spectra between **4** and $[Zn(\mathbf{4})]^{2+}$ in CD_3CN does indicate that complexes are formed in this organic solvent. The lack of complex formation of metal ions with ligand **4** in aqueous solutions is attributed to the steric hindrance imparted by the phenyl substituents in the pyridine 6-positions coupled with the strong solvating ability of water for both the metal cation and the ligand.

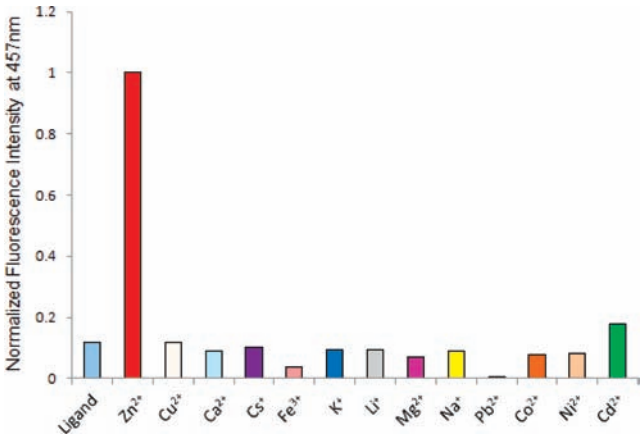

Figure 4. Fluorescence intensity at 457 nm for different metal ions with **3** in CH_3CN. The metal complexes were formed in situ by mixing 1:1 $M(ClO_4)_n$ (M = metal, n = 1, 2, or 3) with ligand **3** at a concentration of 7 μM, and the excitation wavelengths are 300 nm.

Titration of Ligand 3 with Other Metal Ions. Other metal ions were tested by fluorescence titration with ligand **3** in acetonitrile, but none showed spectral shifts as remarkable as those obtained in the case of titration with Zn^{2+} ions (Figure 3, panel B). For instance, when Cu^{2+} was the titrant, the 376 nm fluorescence of compound **3** was quenched by Cu^{2+} without a concomitant increase at 457 nm observed with Zn^{2+}. The binding constant of Cu^{2+} with **3** is estimated to be larger than 10^9 M^{-1} in CH_3CN. Other metals tested included the perchlorate salts of Ca^{2+}, Cs^+, Fe^{3+}, K^+, Li^+, Mg^{2+}, Pb^{2+}, Co^{2+}, Na^+, Ni^{2+}, and Sr^+. Figure 4 shows fluorescene enhancement at 457 nm, where only the Zn^{2+}-complex exhibits strong emission at 457 nm. Even Cd^{2+} showed significant fluorescence quenching at 375 nm but only a weak increase at 457 nm (Figure S6 in the Supporting Information). All other tested metals showed either no change or diminished fluorescence at 376 nm. Metal competition experiments were also carried out and are shown in Figure S7 in the Supporting Information. When the other metal ions listed above were added into the acetonitrile solution of $[Zn(\mathbf{3})]^{2+}$ at ratios of 1:1, 10:1, and 100:1, the emission did not change significantly except that Cu^{2+}, Fe^{3+}, and Ni^{2+} diminished part or all of the red-shifted emission at a 100:1 ratio.

Fluorescence Characteristics of Ligand 3 and Its Complexes with Zn^{2+} Ion. Ligand 3 and Its Subunits. The spectroscopic characteristics of **3** are due to the 6-(3,4,5-trimethoxy-phenyl)-pyridinyl residues which are substituted derivatives of 2-phenylpyridine (2-PhPy). The spectroscopic characteristics of 2-PhPy have been documented.[39−41] The UV absorption bands are almost structureless, and the longest-wavelength band exhibits a maximum at 273 nm in cyclohexane solutions.[40,41] The fluorescence of 2-PhPy is not observable in nonprotic organic solvents but appears with a maximum at 364 nm and with quantum yields of $\sim 10^{-3}$ and 0.13 in ethanol

(35) Anderegg, V. G.; Hubmann, E.; Podder, N. G.; Wenk, F. *Helv. Chim. Acta* **1977**, *60*, 123–140.
(36) Kahmann, K.; Sigel, H.; Erlenmeyer, H. *Helv. Chim. Acta* **1964**, *47*, 1754–1763.
(37) (a) Amicangelo, J. C.; Leenstra, W. R. *J. Am. Chem. Soc.* **2003**, *125*, 14698–14699. (b) De Feyter, S.; Van Stam, J.; Iamns, F.; Viaene, L.; De Schryver, F. C.; Evans, C. H. *Chem. Phys. Lett.* **1997**, *277*, 44–50. (c) Bokobza, L. *Prog. Polym. Sci.* **1990**, *15*, 337–60.
(38) Martell, A. E.; Motekaitis, R. J. *Determination and Use of Stability Constants*, 2nd ed.; VCH Publishers, Inc.: New York, 1992; pp 37−74.
(39) Kubin, J.; Testa, A. C. *J. Photochem. Photobiol.* **1994**, *83*, 91–96.
(40) Sarkar, A.; Chakravorti, S. *J. Lumin.* **1995**, *65*, 163–168.
(41) Deng, F.; Kubin, J.; Testa, A. C. *J. Photochem. Photobiol.* **1997**, *104*, 65–6.

and water, respectively.[40] In 0.1 N H_2SO_4 solution, the emission maximum is also at 364 nm, but the quantum yield is enhanced by a factor of ~5.[39,40] The fluorescence enhancements of 2-PhPy in protic environments are attributed to hydrogen bonding or protonation of the pyridine nitrogen atom in acidic solutions.[40−42] The energy of the nonbonding nitrogen electron pair is thereby lowered, and the fluorescence-emitting $\pi-\pi^*$ state becomes the excited state with the lowest energy instead of the $n-\pi^*$ state.[39]

While the spectroscopic characteristics of ligand **3** are similar to those of 2-PhPy, both the absorption and fluorescence emission maxima are red-shifted (293 and 376 nm, respectively, in CH_3CN). We determined the quantum yield of the fluorescence in CH_3CN by a relative method using quinine sulfate as a standard[43] (quantum yield ~0.012). The spectroscopic characteristics of the compound (2-methyl-6-(3,4,5-trimethoxy-phenyl)-pyridine, **13**), which resembles a single arm of compound **3**, was also examined (Figure S8 in the Supporting Information). The absorption and fluorescence maxima are 292 and 373 nm, respectively, which are close to the values of ligand **3**. These similarities suggest that there are no significant interactions between the three substituted 2-PhPy arms of **3** in the ground state and weak interactions in the excited state since there is only a 3 nm difference in the fluorescence emission maxima between **3** and **13**.

The titration of ligand **3** with sulfuric acid in acetonitrile causes a decrease in its fluorescence intensity (Figure S9 in the Supporting Information). The addition of the first and second equivalent of acid yields decreases of ~15% and ~65% in the fluorescence intensity. The fluorescence maximum does not change significantly and remains at ~375−376 nm until most of the first 2 equiv had been added. The addition of the third equivalent causes a full quenching of the remaining ~20% of the fluorescence and is accompanied by a significant red shift of the emission maximum to about 400 nm. This last step most likely reflects greater protonation of the pyridine nitrogens since such red-shifted emission spectra are characteristic of the pyridinium ion forms of some of the phenylpyridines.[39,40] Addition of acid to **13** results in similarly reduced fluorescence intensity and an even larger red shift. In contrast to **3** and **13**, 2-PhPy increases in fluorescence intensity upon protonation. One explanation is that, in contrast to 2-PhPy, **3** and **13** exhibit $\pi-\pi^*$ excitation and fluorescence even without N-protonation; this effect can arise from the higher energy of the highest occupied molecular orbital (HOMO) of the π system resulting from the electron-releasing alkoxyl substituents. Protonation of **3** and **13** results in a shift of the HOMO and lowest unoccupied molecular orbital (LUMO) orbital energy levels and to the observed changes in the spectra.

Zn(3) Complexes and the One-Armed Control Compound Zn(13). The addition of $Zn(ClO_4)_2$ to acetonitrile solutions of **3** leads to a decrease in the absorbance in the entire spectral region from ~220 to 319 nm and a small increase beyond the isosbestic point at 319 nm (Figure 3A). This hypochromic effect is particularly pronounced within the longest-wavelength 293 nm absorption band and is consistent with enhanced $\pi-$electron interactions between the different arms of the substituted 6-(3,4,5-trimethoxy-phenyl)-pyridinyl residues in the Zn(**3**) complex. These enhanced intramolecular or interarm interactions result from the more compact structure of the Zn(**3**) complexes relative to the more extended structure of the free ligand (parts B and C of Figure 1, respectively) and the shorter distances between the three aromatic nitrogen atoms (N2, N3, and N4) in the Zn(**3**) complex. Upon addition of Zn^{2+}, the 376 nm emission band decreases in intensity and a new emission band with a maximum at 457 nm is observed (Figure 3B). The isoemissive point at 416 nm indicates that the addition of Zn^{2+} transforms the shorter wavelength fluorescent species into a single, longer wavelength-emitting species. The intensity of the 457 nm fluorescence band increases with increasing concentration of Zn^{2+} and saturates after 1 equiv has been added. However, the 376 nm fluorescence band does not disappear completely and manifests itself as a shoulder on the short wavelength side of the new 475 nm band even in the presence of an excess of Zn^{2+}. Diluting the solution by a factor of 10 does not change the qualitative aspects of these spectroscopic characteristics (data not shown). The excitation spectra of the 375 and 457 nm fluorescence emission bands are practically identical when viewed at either the 375 or 457 nm emission bands for the ligand **3** and its Zn(**3**) complex (Figure 3C). This indicates that the initial excited state relaxes to a lower energy fluorescence emitting state in the case of the Zn(**3**) complex than in the ligand **3**.

Addition of Zn^{2+} (0−35 μM) to the single-armed control compound **13** (Scheme 1) yields entirely different results than in the case of the three-armed **3** in acetonitrile (Figure S8 in the Supporting Information). The UV absorbance maximum at 290 nm diminishes and shifts 2−3 nm to the red in the $[Zn^{2+}] = 0-8\ \mu$M range, and a prominent new and red-shifted absorption band develops with a broad maximum at 340 nm. A well-defined isosbestic point is evident at 308 nm (Figure S8A in the Supporting Information). The fluorescence excitation spectra demonstrate that the new red-shifted band does not generate any fluorescence, while excitation within the unshifted UV absorption band at 290−293 nm produces a normal fluorescence with a maximum at 373 nm, same as ligands **13** or **3** in the absence of Zn^{2+} ions. While we did not further investigate the nature of the new absorption band at ~340 nm in the Zn(**13**) complex, we conclude that the red-shifted fluorescence emission band in the case of the Zn(**3**) with a maximum at 457 nm (Figure 3B) is a result of the structure, impact, and interactions between the three arms in the excited state of the Zn(**3**) complex. While similar red-shifted absorption bands as in the Zn(**13**) complexes have been observed in Zn^{2+} complexes with other terpyridine[6,7] and bipyridyl derivatives,[2] in most cases red-shifted fluorescence emission spectra were also observed. These red-shifted emission spectra were attributed to a planarization of the two pyrimidyl rings in the bipyridyl metal ion-bound fluorophore[2] or to intramolecular charge transfer complex formation.[6,7]

(42) Deng, F.; Kubin, J.; Testa, A. C. *J. Photochem. Photobiol.* **1998**, *118*, 1–6.
(43) Ware, W. R.; Rothman, W. *Chem. Phys. Lett.* **1976**, *39*, 449–453.

Fluorescence Decay Profiles. Representative time-resolved fluorescence decay profiles (300 nm picosecond laser pulse excitation) of the control compound **13** (panel A), ligand **3** (panel B), and the Zn(**3**) complex (panel C) are shown in Figure 5. The fluorescence decay curves ($I_F(t)$) of the free control compound **13** and Zn(**13**) complexes measured at an emission wavelength of 370 nm are not distinguishable from one another (data not shown) within experimental error and can be described in terms of a single-exponential decay function $I_F(t) = A \exp[-t/\tau]$ with amplitude A and lifetime $\tau = 1.50 \pm 0.1$ ns (based on three independent measurements). On the other hand, the fluorescence decay profile of ligand **3** with three 6-(3,4,5-trimethoxy-phenyl)-pyridinyl arms is nonexponential but is well described in terms of a sum of three exponentials components:

$$I_F(t) = A_1 \exp[-t/T_1] + A_2 \exp[-t/T_2] + A_3 \exp[-t/T_2] \quad (1)$$

The three components have lifetimes τ_1, τ_2, τ_3, with amplitudes A_1, A_2, and A_3, respectively. The amplitude-weighted average lifetime is $\tau_{AV} = A_1 \tau_1 + A_2 \tau_1 + A_3 \tau_1$ and has values of 0.36 ns when the fluorescence decay curve is monitored at 378 nm and 0.63 ns when it is monitored at the red edge of fluorescence band at 456 nm. (Details are shown in Table S1 in the Supporting Information.) The wavelength dependence of τ_{AV} and the nonexponential fluorescence decay of ligand **3** is a manifestation of a conformational heterogeneity of fluorophores. The wavelength-dependence τ_{AV} signifies that the fluorescence emission spectra are also heterogeneous with the longer wavelength-emitting forms having a longer lifetime than the shorter-wavelength emitting ones. Such behavior has been reported for other fluorophores such as twisted intramolecular charge transfer states[44] and is therefore not unusual. Each of the three amplitudes, A_1, A_2, and A_3, are proportional to the fractions of molecules excited at 300 nm that decay with lifetimes of τ_1, τ_2, and τ_3 (assuming that the molar absorptivities of each conformationally distinct component are similar for each). These fractions most likely represent different ground state conformers of ligand **3**, and such a heterogeneity is consistent with the open flexible structure of **3** (Figure 1C). We note that heterogeneity of lifetimes indicates that different conformers are not in exchange with one another on the nanosecond time scale of the experiments in Figure 5. This result is therefore not in contradiction with the interpretations of the NMR data associated with Figure 2.

The fluorescence decay profiles of Zn(**3**) complexes are also heterogeneous and can be interpreted using eq 1. At the short-wavelength edge of the red-shifted fluorescence band measured at its short-wavelength edge at 378 nm (Figure 3B), the most prominent component has an amplitude of 65.5% and a lifetime of 2.0 ns, while the other two components have lifetimes of 0.18 (24.6%) and 4.0 ns (9.9%), with $\tau_{AV} = 1.8$ ns. However, when measured at the emission maximum of 456 nm, the value of $\tau_{AV} = 3.5 \pm 0.1$ ns is significantly longer than the value of 0.36 ns measured at the 378 nm emission maximum of ligand **3** (Table S1 in the Supporting Information). The ratios of these τ_{AV} values are ~10, which is consistent with the differences in the steady-state fluorescence yield for the free ligand **3** and its Zn complex, Zn(**3**), shown in Figure 3. The heterogeneous decay profiles with individual lifetimes < 5 ns indicate that the different conformers of the Zn(**3**) complexes exchange on time scales that are greater than > 5 ns; a rapid exchange would give rise to a single fluorescence decay component.

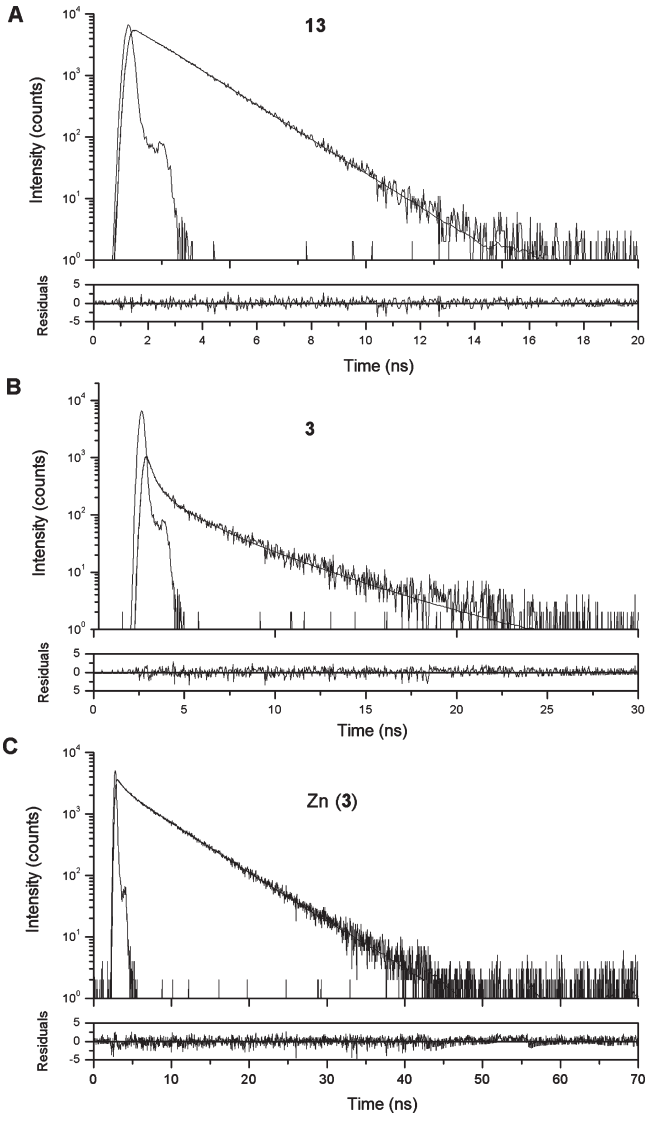

Figure 5. Time resolved fluorescence decay profiles. The fits of eq 1 (with the experimental parameters summarized in Table S1 in the Supporting Information) to the experimental data points is superimposed on the data points and is discernible only near the end of the decay curves. The residuals are shown at the bottom of each point, and the differences between the computed and experimental data points do not exceed ±5 counts. (A) 7 μM **13** in CH_3CN, emission wavelength 370 nm; $\chi^2 = 0.78$. (B) 7 μM ligand **3** in CH_3CN, emission wavelength 456 nm; $\chi^2 = 0.67$.(B) 7 μM Zn(**3**) in CH_3CN, emission wavelength 456 nm; $\chi^2 = 0.74$.

Comparisons with Other Complexes Involving the Coordination of Zn^{2+} with Nitrogen Atoms in Other Heterocyclic Aromatic Ring Ligands. Although our Zn(**3**) complexes display many of the same spectroscopic characteristics as some of the other Zn−ligand complexes that have been studied,[1a,2−6,8,9] the Zn(**3**) complexes have

(44) Köhler, G.; Rechthaler, K.; Rotkiewicz, K.; Rettig, W. *Chem. Phys.* **1996**, *207*, 85–101.

some very unique features: (1) The coordination with Zn^{2+} leads to a significant structural rearrangement in which the three 6-(3,4,5-trimethoxy-phenyl)-pyridinyl arms are in a much closer contact with one another than they are in the free ligand **3** (Figure 1B,C). (2) The fluorescence decay profiles are monoexponential in the case of ligand **13** and multiexponential in the case of free ligand **3**, indicating a heterogeneity of conformers in the latter (Figure 5). (3) The presence of the three substituted 2-Ph-Py arms in **3** play an important role in the coordination of Zn^{2+} ions by ligand **3** that helps to stabilize the trigonal bipyramidal geometry of the Zn(**3**) complex. (4) The absence of two of the ligand arms in the Zn(**13**) (or Zn(**2-PhPy**) complexes[39−42]) not only weakens the binding of Zn^{2+} ions to ligand **13** (Figure S8A,B in the Supporting Information) but also changes the properties of the excited state relative to those of the Zn(**3**) complex.

Possible Origins of the Red-Shift in the Fluorescence Emission Spectrum of the Zn(3) Complex. The UV absorption features of the three-armed free ligand **3**, the one-armed ligand **13**, and the Zn(**3**) and Zn(**13**) complexes are all similar to one another. However, substantial differences manifest themselves in the fluorescence characteristics of the Zn-coordinated three-armed Zn(**3**) and single-armed Zn(**13**) complexes (Figure 3A,B and Figure S8A,B in the Supporting Information). The binding of Zn^{2+} ions to **3** enhances the electronic interactions of each of the three arms of **3** with one another.[45] These interactions are weak in the ground state since the UV absorbance spectra of **3** and **13** are similar (Figure 3A and and Figure S8A in the Supporting Information). In the excited state, however, the phenylpyridinyl moieties are physically close to one another (Figure 1C) and electronic interactions between them by an exciton-type interaction can contribute to the observed red shift in the fluorescence emitting spectrum.[37] On the other hand, in the excited state, a decrease in the twist angles between the trimthoxyphenyl and pyridyl rings can lead to a greater planarization[2] and thus greater $\pi-\pi^*$ character[39] of the excited state of the Zn^{2+} ion−coordinated ligand **3**. Such an effect can also cause a red shift in the fluorescence spectrum. However, since the red-shifted fluorescence spectrum of Zn(**3**) complexes is structureless in all solvents, the $\pi-\pi^*$ character of the excited state[39] seems rather weak. Broad, red-shifted fluorescence emission spectra are often the hallmark of charge-transfer states. We observe a weak effect of solvent polarity on the wavelength of the red-shifted fluorescence emission maximum (Figures S11−S13 in the Supporting Information). The fluorescence maximum occurs at the shortest wavelength (412 nm) in diethyl ether which has the lowest dielectric constant (4.3), at intermediate wavelengths in chloroform and dichloromethane (ε = 4.9 and 9.1, respectively), and at the longest wavelength (457 nm) in acetonitrile (ε = 37). A charge-transfer (CT) interaction in Zn(**3**) complexes involves the donor trimethoxyphenyl and the pyridyl acceptor moiety in ligand **3**. The coordination of Zn^{2+} increases the electron acceptor capacity of the pyridyl group, which has been observed in other systems[45] and provides the rationale for the observed weak solvent effect on the fluorescence emission maxima which is expected for CT states with weak dipole moments.[46] In the case of the Zn(**3**) complex, we expect that the dipole moment due to charge separation would develop along the long axis joining the tips of the pyramids (the N1−Zn−N5 direction in Figure 1B). The UV absorption band with a broad maximum at 340 nm that develops when the one-armed pyridyl-trimethoxyphenyl derivative **13** is titrated with $Zn(ClO_4)_2$ in acetonitrile (Figure S8 in the Supporting Information) has been tentatively attributed to a CT state (see above). The fluorescence of this CT state is strongly quenched (Figure S8C in the Supporting Information), probably by an efficient internal conversion mechanism that is associated with rotation about the bond joining the trimetroxyphenyl and heterocyclic aromatic rings in the Zn(**13**) complexes. Such a rotation should be significantly more hindered by the close proximity of the three arms of the ligand **3** in the Zn(**3**) complex, thus favoring the decay of the excited state by fluorescence.

Conclusions

Two soluble triphenyl substituted TPA derivatives were prepared. Even though compound **2** is barely soluble in most common solvents, compound **3** is soluble in organic solvents, and compound **4** is soluble in both aqueous and organic solvents. The X-ray structures of ligand **3** and two zinc complexes ($[Zn(\mathbf{2})(CH_3CN)](ClO_4)_2$ and $[Zn(\mathbf{3})(CH_3CN)](ClO_4)_2$ show that the three aromatic arms of the ligand fold upon metal ion complexation to form a hydrophobic cavity with the size of about an acetonitrile molecule. Binding studies suggest weak metal ion coordination with compound **4** in aqueous media. Binding studies in organic solution by fluorescence and NMR spectra showed that compound **3** had moderate affinities for metal ions such as Zn^{2+} and Cu^{2+}. The reduced affinities compared to TPA (**1**) result from steric and electronic effects of the substituents. Ligand **3** showed a red-shifted fluorescence response to Zn^{2+} in CH_3CN upon Zn^{2+} coordination, while no other metal ions studied showed such behavior. Detailed photophysical studies indicate that the ~80 nm red shift in the fluorescence emission spectrum of the Zn^{2+} ion-coordinated ligands in the Zn(**3**) complex is consistent with an excited state with charge-transfer character and/or a less twisted conformation of the two substituted aromatic rings of the pyridyl-trimethoxyphenyl groups, or possibly excitonic interactions.

Acknowledgment. This work was supported financially by the National Science Foundation (Grant CHE-0848234) and the National Institutes of Health (Grant GM-076202). We thank William W. Brennessel of the X-ray Crystallographic Laboratory at University of Minnesota (Minneapolis, MN). This work was supported in part by Research Facilities Improvement Grant Number C06 RR-16572 from the NCRR/NIH. Instrumentation was purchased with support from NSF Grants CHE-0234863 and CHE-0116222.

Supporting Information Available: Synthesis of **5**, additional NMR, fluorescence, and potentiometric titration data, and CIF files for $[Zn(\mathbf{2})(CH_3CN)](ClO_4)_2$, $[Zn(\mathbf{3})(CH_3CN)](ClO_4)_2$, **3**, and $[H(\mathbf{3})]ClO_4$. This material is available free of charge via the Internet at http://pubs.acs.org.

(45) Li, Y. Q.; Bricks, J. L.; Resch-Genger, U.; Spieles, M.; Rettig, W. *J. Phys. Chem. A* **2006**, *110*, 10972–10984.

(46) Grabowski, Z. R.; Rotkiewicz, K. *Chem. Rev.* **2003**, *103*, 3899–4031.